

Water Resources Research

RESEARCH ARTICLE

10.1029/2018WR024486

Key Points:

- Weather, hydrological, biochemistry, and anthropogenic conditions control organic-sediment interactions and dynamics in river water
- Dry weather condition enhances production of aquagenic organic matter and flocculation-deposition of particulate matter in river water
- High rainfalls facilitate transportation of terrigenous humic substances and stabilization-resuspension of particulate matter

Correspondence to:

B. J. Lee,
bjlee@knu.ac.kr

Citation:

Lee, B. J., Kim, J., Hur, J., Choi, I. H., Toorman, E., Fettweis, M., & Choi, J. W. (2019). Seasonal dynamics of organic matter composition and its effects on suspended sediment flocculation in river water. *Water Resources Research*, 55, 6968–6985. <https://doi.org/10.1029/2018WR024486>

Received 23 NOV 2018

Accepted 1 AUG 2019

Accepted article online 6 AUG 2019

Published online 19 AUG 2019

Seasonal Dynamics of Organic Matter Composition and Its Effects on Suspended Sediment Flocculation in River Water

B. J. Lee¹ , J. Kim¹, J. Hur², I. H. Choi³, E. A. Toorman⁴ , M. Fettweis⁵ , and J. W. Choi¹

¹Department of Disaster Prevention and Environmental Engineering, Kyungpook National University, Sangju, South Korea, ²Department of Environment and Energy, Sejong University, Seoul, South Korea, ³Water Analysis and Research Center, K-water, Daejeon, South Korea, ⁴Hydraulics Laboratory, Department of Civil Engineering, Katholieke Universiteit Leuven, Leuven, Belgium, ⁵Operational Directorate Natural Environment, Royal Belgian Institute of Natural Sciences, Brussels, Belgium

Abstract Organic matter (OM) and suspended sediment are abundant, and interact with each other, in rivers and lakes. OM is usually adsorbed by suspended sediment and causes either particle stabilization or flocculation. In this study, the OM composition and suspended sediment flocculation potential of river water were regularly measured throughout the year 2016. The OM composition of the river water samples was measured with a liquid chromatography-organic carbon detection system and fluorescence excitation-emission matrix spectroscopy, and the flocculation potential was measured in a standard jar test experiment. Results from the OM analyses and flocculation potential tests, in association with a multivariate data analysis, demonstrated that the OM composition and flocculation potential of the river water were dynamic under different meteorological, hydrological, ecological, and anthropogenic conditions and closely correlated with each other. Dry seasons with low rainfall and water discharge induced a lacustrine condition and led to the OM composition being more aquagenic and flocculation-favorable. The most favorable condition for the enhancement of flocculation was during algae bloom and associated with the production of biopolymers from algae. In contrast, rainy seasons were advantageous for stabilization of suspended sediment because of excessive transport of terrigenous humic substances from catchment areas into the river. Such terrigenous humic substances enhanced stabilization by creating enhanced electrostatic repulsion via adsorption onto the sediment surface. Findings from this research provide a better insight into the highly complex behaviors of and interactions between OM and suspended sediment in natural water environments.

1. Introduction

Suspended sediment (SS) in surface water bodies comprises a mixture of clay to sand-sized particles in suspension. Varying amounts of minerals and organic matter (OM) comprise SS. The minerals have physicochemical (e.g., clay minerals, quartz, and feldspar) and biogenic origin (e.g., calcite, aragonite, and opal). The particulate OM consists of living (e.g., bacteria, phytoplankton, and zooplankton) and nonliving species (e.g., fecal and pseudo-fecal pellets, detritus and its decomposed products from microbial activity, such as mucus and exopolymers), as well as xenobiotic particles from human activities (e.g., microplastics). This combination of clays, minerals, and OM is also referred to as cohesive sediments because of their cohesive property in aqueous suspension (Partheniades, 2009). Obvious effects of SS in the water column are a decrease in water clarity and the occurrence of muddy deposits. Because of the high specific surface area and reactivity, SS can also adsorb a large amount of chemical contaminants, such as hydrophobic organic pollutants and (heavy) metals, and hence threaten water environments (Capuzzo et al., 2015; USEPA, 2002; Wisser et al., 2013).

OM and SS are substantial ingredients in water resources. The fine-grained sediment particles in the SS are originally generated by the weathering of soils and rocks and are discharged into rivers and streams, from where they eventually reach the sea and the oceans. These particles are kept in suspension and are transported by turbulence and water flow. OM has its terrigenous and autochthonous origins (Bade et al., 2007; Kritzberg et al., 2004; Rautio et al., 2011). Terrigenous OM is transported from the catchment areas during

periods with high rainfall and discharge into the river, whereas autochthonous OM is produced in situ by aquatic organisms. Humic substances (HS) and polysaccharidic extracellular polymeric substances (EPS) are typical chemical species of terrigenous and autochthonous OM, respectively. OM undergoes various biochemical reactions in the water. It is important to note that OM attaches to the SS and modifies its surface properties. Changes in the OM quantity and quality influence the fate and transport of the SS in seasonal or longer periods. For example, climate change tends to increase water temperature, algae growth and autochthonous OM production, which are conducive to biologically mediated aggregation and deposition of SS (Kondolf et al., 2014; Kondolf & Wilcock, 1996).

The physicochemical process causing SS to aggregate into large settleable flocs is referred to as flocculation (Maggi, 2005; van Leussen, 1994). On the other hand, stabilization is defined as the counteraction of flocculation, which hinders particle attachment and aggregation and promote floc breakage (Fleer et al., 1993; B. J. Lee, Schlautman, et al., 2012). Flocculation and stabilization determine the floc size and settling velocity of SS, and thus controls the overall fate and transport of these sediments. Besides the water chemistry, like ionic strength, EPS, produced by aquatic organisms, can enhance flocculation. The chain-like molecular structures of EPS bind particles together in large settleable flocs. High EPS concentration, triggered by algae blooms, has been reported to intensify flocculation of SS in fresh, estuarine, and marine water environments (M. S. Chen et al., 2005; Fettweis & Baeye, 2015; B. J. Lee, Fettweis, et al., 2012; B. J. Lee et al., 2017; W. T. B. van der Lee, 2000). The mixture of EPS, microorganisms, and SS that is often found in eutrophic water conditions can lead to the formation of so-called bio-mineral flocs, which eventually settle and deposit on river or lake beds (Droppo, 2001; Larsen, Harvey, & Crimaldi, 2009; Larsen, Harvey, Noe, et al., 2009; Maggi, 2009, 2013; Maggi & Tang, 2015; Tang & Maggi, 2016; Zimmermann-Timm, 2002).

EPS is not the only OM in surface water bodies. OM consists of a variety of many other small and medium-sized organic compounds, such as intracellular and extracellular macromolecules and HS (Hudson et al., 2007; Sillanpaa et al., 2018). Previous studies investigated both OM-mediated flocculation and stabilization in aqueous suspensions under special physical and biochemical conditions (Kretzschmar et al., 1998; Labille et al., 2005; Leng et al., 2002; Wilkinson et al., 1997). Furukawa and coworkers also demonstrated the respective roles of HS and EPS on flocculation and stabilization in fresh and saline water suspensions (Furukawa et al., 2014; Tan et al., 2012; G. Zhang et al., 2013). The findings of the earlier studies indicate that OM may be adsorbed across the large surface areas and reactive sites of suspended sediment. The adsorbed OM can modify the surface properties of suspended sediment in a way that enhances either repulsion or attraction between particles (i.e., stabilization or flocculation). For example, the HS, with their relatively low molecular weights (up to several thousand grams per mole), promote stabilization of suspended particles via their coating onto the surface area and by increasing the electrostatic repulsion between particles (Kretzschmar et al., 1998; Wilkinson et al., 1997). On the other hand, EPS in the form of long-chain polymeric substances with high molecular weights bind SS together and enhance flocculation, as they are large enough to reach other particles outside of the electrostatic repulsive layer of SS (Fleer et al., 1993; B. J. Lee & Schlautman, 2015).

The earlier researchers, listed in the paragraph above, however, tested and proved their hypotheses in idealized laboratory experiments, disregarding the dynamics of and the interactions between OM and SS in natural water environments. Lee and coworkers recently attempted to investigate the seasonal dynamics of OM composition and OM-mediated flocculation in river water, demonstrating the dominance of stabilization in river water with many HS during rainy seasons, and of flocculation with many EPS during algae blooms (B. J. Lee et al., 2017). However, the dynamics of and the interactions between OM and SS are highly complex and remain poorly understood in natural water environments. More attention and efforts are required to identify the environmental factors determining OM and SS dynamics, and to elucidate the causal relationship between OM composition and OM-mediated flocculation.

Climate change has been a serious stressor to water resources in recent years through changes in rainfall and increasing temperatures that can also change the hydrological, ecological, and biochemical conditions of water bodies. The consequences of these perturbations are changes in the amount and composition of OM and SS, and thus of their dynamics. Further, various dam construction works, coping with the scarcity of water resources from an economic and engineering perspective, can often also result in sudden changes in hydrological, ecological, and biogeochemical conditions, thus influencing the OM and SS. The overall

connectivity, from the natural and anthropogenic stressors to the hydrobiochemical conditions, and then to the OM and SS dynamics, has not yet been fully understood. This research thus aims to elucidate the causal relationship between the environmental factors, encompassing meteorological, hydrological, biochemical, and anthropogenic stressors, and the OM and SS dynamics, in water resources, focusing on biologically mediated flocculation. This study will help improve understanding regarding the highly complex behaviors of OM and SS in natural water environments and help provide information needed to maintain good water and sediment quality of water resources.

2. Materials and Methods

2.1. Study Site and Sampling

The study site was located in the Nakdong River, a major river and river basin in southeastern Korea with a drainage area of 23,384 km² (Figure 1). The river and the river basin have seasonal variation in terms of the meteorological, hydrological, and ecological conditions. The water temperature of the river ranged from 5 to 30 °C throughout the year of the study. Rainfall and discharge in the river basin also change seasonally with a rainy season in summer and a dry season in winter. The movable weirs in Nakdong River were constructed in 2011 and have been in operation until the present day (Jun & Kim, 2011; Lah et al., 2015). A tributary (Geumho River) that passes through Daegu Metropolitan City is located upstream of the study site, and hence contributes a large amount of organic pollutants and nutrients to the Nakdong River.

From January to December 2016, water samples were collected weekly or biweekly during algae blooms in summer, and monthly during normal periods, at sampling points found in the river section between two weirs (Figure 1). At W2, a 40-L water sample, large enough to perform experiments and chemical analyses, was collected at each field campaign, immediately upstream of the Dalsung weir, with a water depth sampler (Changshin Science, Korea), at 1 m below the surface to avoid sampling of floating matter. Water quality parameters, such as pH, temperature, and dissolved oxygen, were measured on site with Manta Multiprobes (Eureka Inc, Austin, USA). Then, the water samples were transported to the laboratory close to the study site and filtered through 1.2- μ m pore size GF-C filter paper (Hyundai Micro, Korea) to exclude algae and other particulate matter, while retaining mostly submicron-sized OM. Then, the filtered and unfiltered raw water samples, retaining OM only and OM with algae, respectively, were used for the flocculation potential tests. Hereinafter, flocculation potential represents the physical, biochemical status of river water that enhances particle attachment, aggregation, and sedimentation.

In addition, water quantity (e.g., flow rate) and quality (e.g., temperature, pH, dissolved oxygen (DO), total phosphorus (TP), and blue-green algae (BGA) cell number concentration) data from two national monitoring stations in the study site (M1 and M2 in Figure 1) were downloaded from publicly accessible websites (www.wamis.go.kr and water.nier.go.kr). Flow rate was monitored at the M1 station, based on a rating curve between water depth and flow rate. BGA cell number concentration was measured with a cell counting method (Joung et al., 2006; Korea Ministry of Environment, 2016). Annual rainfall intensity data were collected from the M1 monitoring station.

2.2. Flocculation Potential Test

Flocculation potential tests of the filtered and unfiltered river water samples were performed using a standard jar tester (MS-SF6, Misung, Korea; B. J. Lee et al., 2017; B. J. Lee & Schlautman, 2015). Duplication of the tests with the filtered and unfiltered water samples was purposed to investigate the effect of EPS bound to algal cells or particulate biomass on flocculation potential. Kaolinite (Sigma-Aldrich, MO) was used as the model clay particle in the tests, because it is one of the most abundant clay species in the study site and has been widely used in earlier studies (Kretzschmar et al., 1998; B. H. Lee & Jeong, 2008; B. J. Lee, Schlautman, et al., 2012; Mietta, Chassagne, & Winterwerp, 2009). Before the start of the test, a kaolinite stock suspension was prepared at 20 g/L. The ionic strength and pH of the kaolinite stock solution were adjusted at 0.001 M NaCl and 7.0, respectively. The kaolinite stock solution was added at different volumes to the six jars of the jar tester, and a filtered or an unfiltered river water sample was added to fill the 2-L volume of each jar. This resulted in the kaolinite concentrations of the six jars being 0.1, 0.2, 0.5, 1.0, 1.5, and 2.0 g/L. Note that the jar test was duplicated for the filtered and unfiltered river water samples. Afterward, the mixtures of the kaolinite suspension and the filtered or unfiltered river water sample were mixed rapidly

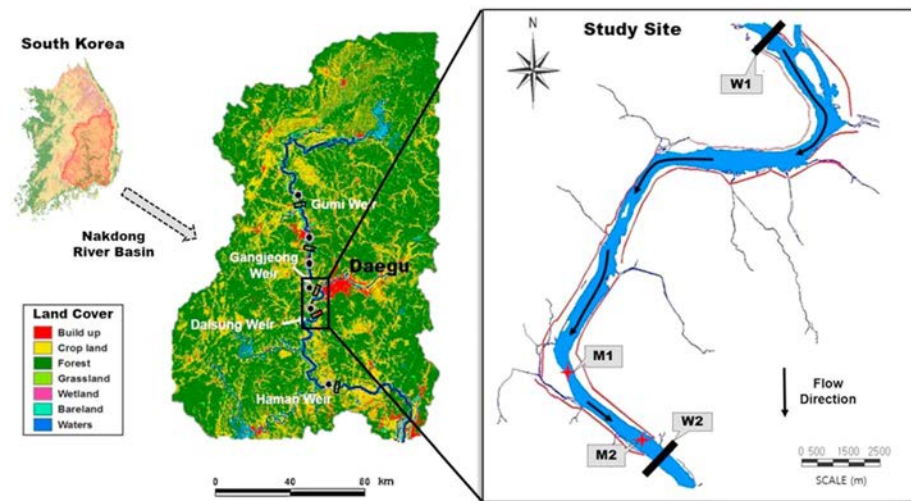


Figure 1. Map of the study site, including a section of the Nakdong River from the Goryeong weir to the Dalsung weir. The W1 and W2 points on the map represent the Goryeong weir and the Dalsung weir, respectively. Water sampling and measurement campaigns were performed at the W2 point. The M1 and M2 points indicate the national monitoring stations for water quantity and quality.

at 200 rpm ($G \approx 250/s$) for 2 min to homogenize the mixture, and stirred slowly at 50 rpm ($G \approx 45/s$) for 6 hr to promote flocculation and to obtain a steady state. Previous flocculation kinetic studies have shown that flocculation kinetics in clay suspension reach steady state within a few hours (Furukawa et al., 2014; Mietta, Chassagne, Manning, et al., 2009; Mietta, Chassagne, & Winterwerp, 2009). Because flocculation potential tests in this study were performed with higher suspended solid concentrations (0.1–2.0 g/L) than those of the earlier flocculation kinetic studies (≈ 0.1 g/L), they might reach the steady state sooner. After the 6-hr stirring, the suspended floc sizes were measured. After an additional 1 hr of settling without stirring, an aliquot of the supernatant was taken from each jar to determine the residual solids concentration in the water column above the kaolinite deposit.

Suspended flocs were sampled from the jar tester with a spatula and immediately fixed on a liquefied agar plate (Gorczyca & Ganczarczyk, 1996; B. J. Lee et al., 2017; B. J. Lee, Schlautman, et al., 2012). The plate was then cooled to room temperature (25 °C) to solidify the gel and prevent further changes to the floc structure. Microscope images of the fixed flocs were recorded with a Sony Alpha 6000 camera, equipped with a Sony 30 mm f3.5 macro lens. A public domain image processing software package (Image J, National Institutes of Health, MD) was used to process the raw floc images and calculate the average floc diameter of the circle of equal area (D50; Heywood diameter). It is important to note that the D50 that we calculated in this paper do not fully reflect the entire range of particle sizes, because the minimum measurable floc size was set at 20 μm due to the resolution limit of the camera. The process of sampling, fixing, and imaging flocs was replicated 3 times for each jar test. D50 was used as an indicator of the flocculation potential for each test condition. In addition, as a flocculation potential index, residual solids concentrations were determined following Standard Methods 2540D, Total Suspended Solids (APHA, 1998). Each sample aliquot taken after an hour of settling was filtered through a preweighed 0.2- μm membrane filter (Hyundai Micro, Korea). Then, the filter with its collected solids was dried at 105 °C, reweighed, and the mass of collected solids was determined as the difference in weight. Normalized ratios of the suspended solids concentration after the 6-hr stirring and 1-hr settling against the total initial concentration in the water column (C/C_0) was estimated as an indicator of the flocculation potential, as it correlates with floc size and settling velocity. The detailed measurement procedures for the flocculation potential indices can be found in earlier articles (B. J. Lee et al., 2017; B. J. Lee, Schlautman, et al., 2012).

2.3. Measurement of OM Characteristics

A liquid chromatography-organic carbon detection (LC-OCD) system (DOC Labor Dr. Huber, Karlsruhe, Germany), consisting of a chromatographic column with organic carbon and ultraviolet detectors

(OCD and UVD), was employed to measure the molecular size distributions of OM in water samples (M. Chen et al., 2016; Huber et al., 2011; Huber & Frimmel, 1994). The LC-OCD system in this study was specifically aimed to quantify the key OM components, which are polysaccharidic biopolymers and humic substances, based on their molecular size distributions. Polysaccharidic biopolymers usually have large molecular size and increase flocculation by bridging particles, whereas humic substances have relatively small molecular size and enhance stabilization by coating particles with additional repulsive electrostatic force. A mobile phase containing a phosphate buffer at pH 6.85 was used, and the flow rate was maintained at 1.1 ml/min. An aliquot (1 ml) of the sample was injected into the instrument and filtered through a 0.45 μm in-line PES filter (Sartorius, Germany) prior to the chromatographic column and the OCD and UVD detectors. Thus, the LC-OCD quantified dissolved and colloidal OM with the sizes less than 0.45 μm , while they were found to be informative enough to distinguish seasonal variation in OM composition. Injecting a river water sample (1 ml) through the chromatographic column allows for separation of the OM, depending on the molecular size. While traveling through the chromatographic column, small OM eluted later than larger OM, because it was trapped and retarded in the porous packing material of the column. For calibration of molecular weights, Suwannee River humic and fulvic acids, obtained from the International Humic Substances Society (IHSS), were used (Huber et al., 2011). A built-in software package (ChromCALC) was then used for acquisition and processing of chromatographic data and quantification of different size fractions, including biopolymers ($\text{MW} > 20,000$ Da), humic substance (HS) ($1,000 < \text{MW} < 20,000$ Da), building blocks ($300 < \text{MW} < 500$ Da), and low molecular weight (LMW) neutrals and acids ($\text{MW} < 350$ Da). Comparing both the chromatographic data from the OCD and UVD could measure additional OM characteristics, such as molecularity and aromaticity.

For fluorescence excitation-emission matrix spectroscopy coupled with parallel factor analysis (EEM-PARAFAC), the samples were adjusted to pH 3 by adding 1 M HCl prior to the measurements, which minimizes the potential interferences from pH variation and metal binding. UV absorption coefficient at 254 nm (UV₂₅₄) was measured with a Hach DR5000 UV-visible spectrophotometer (Hach, USA), with Milli-Q water as the blank. SUVA was calculated by dividing 100-fold UV absorbance at 254 nm with dissolved organic carbon (DOC), which serves as a rough estimate of aromatic dissolved OM (Weishaar et al., 2003). The EEMs of the samples, diluted until $\text{UV}_{254} < 0.05 \text{ cm}^{-1}$, were scanned using a Perkin-Elmer LS-55 luminescence spectrometer over excitation/emission wavelengths of 250–500 nm and 280–550 nm at increments of 5 nm and 0.5 nm, respectively. The EEM of each sample was treated by blank subtraction and normalization using a Raman peak of Milli-Q water excited at 350 nm. The EEM spectra of the river water samples were subjected to PARAFAC modeling, using MATLAB software with the DOMFluor toolbox. The detailed procedures of the EEM-PARAFAC can be found elsewhere (Hur & Cho, 2012; Yang, Han, et al., 2015; Yang, Hur, et al., 2015).

2.4. Redundancy Analysis

Redundancy analysis (RDA), a multivariate ordination analysis, was used to examine the variation in a set of environmental variables that can be denoted by a set of descriptive variables (Buttigieg & Ramette, 2014; Legendre & Legendre, 1998; Palmer et al., 2011; Rametter, 2007; ter Braak & Prentice, 2004; Ye et al., 2009). The RDA was specifically used to examine the relationship between the flocculation potential descriptors and the hydrological and water quality variables and was also applied to investigate the seasonal variation of the physical and biochemical status of river water. The RDA was performed with the statistical programming software R (v3.3.2), using the functions “rda” and “plot” from the package “vegan” (Oksanen et al., 2019). The flocculation potential descriptors are floc size and residual solid concentration (see section 2.2), and the variables are the quantities of the OM components obtained from the EEM-PARAFAC and the LC-OCD analyses as well as the hydrological and water quality indices.

3. Results and Discussion

The samples taken during the year 2016 allowed us to investigate how the measured parameters varied in different seasons, with respect to the weather and hydrological conditions. The summer rainy season occurred in July, followed by a second period with high rainfall and discharges in September and October (Figure 2a). The second rainy period in fall was unusual for the study site, compared to the typical weather condition for that time. The water temperature ranged between 4 and 32 °C throughout the year, and

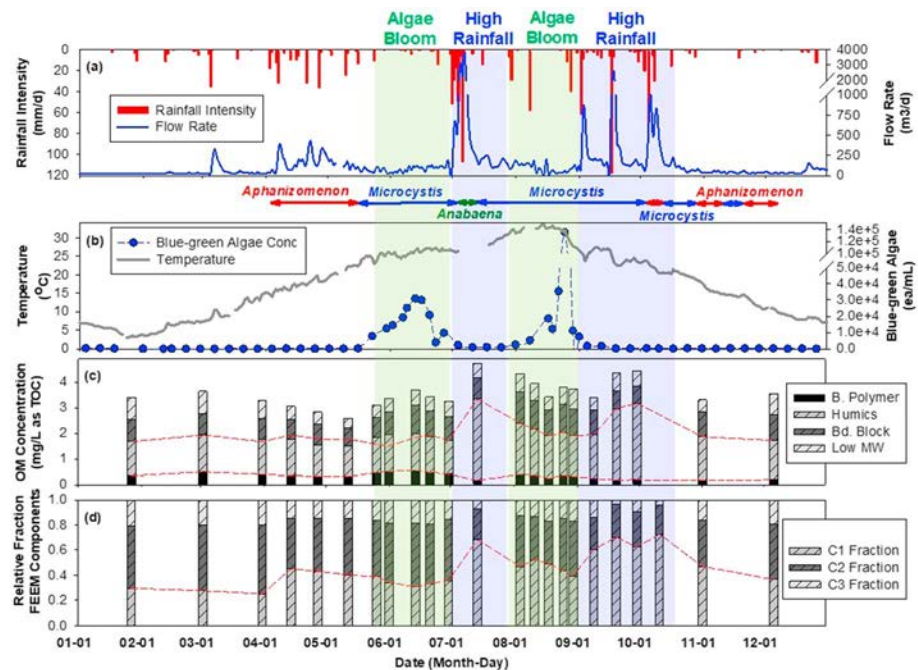


Figure 2. Seasonal variations of the weather, hydrological, and ecological conditions, and the organic matter (OM) composition. The respective panels represent the yearly plots of (a) rainfall intensity and flow rate, (b) water temperature and blue-green algae number concentration, (c) OM concentrations of biopolymers ($MW > 20,000$ Da), humic substance ($1,000 < MW < 20,000$ Da), building blocks ($300 < MW < 500$ Da), and low molecular weight neutrals and acids ($MW < 350$ Da), which are indicated by B. polymer, Humics, Bd. Block, and Low MW, respectively, in the legend, and (d) OM fractions of the humic-like C1, tyrosine-like C2, and tryptophan-like C3 components.

remained above 25°C from July to September. The warm and sunny weather condition in the summer facilitated algae blooms in June and August, which were attenuated by the subsequent high rainfall and discharge (Figure 2b). These variations in the weather, hydrological, and ecological conditions were found to control the seasonal dynamics of the OM composition and flocculation potential of the river water (Figures 2c and 2d), as will be discussed closely in the following sections.

3.1. Flocculation Versus Stabilization

Figure 3 shows representative results from both the flocculation- and stabilization-dominant cases, in which the flocculation potential indices (i.e., D_{50} as the average floc diameter of the circle of equal area and C/C_0 as the normalized ratios of the residual solids concentration against the total concentration in the water column) were plotted against kaolinite dose concentration. The D_{50} floc size generally decreased with increasing kaolinite dose concentration in each jar test experiment, indicating a tendency for larger and looser flocs to form at a lower kaolinite concentration, and smaller and more compact flocs at a higher kaolinite concentration. The low kaolinite concentration for a given amount of EPS in our water samples led to larger and more fluffy flocs, similar to marine snow (Bainbridge et al., 2012; Fettweis & Lee, 2017). D_{50} further decreased and approached the measurement threshold (i.e., $20\ \mu\text{m}$) at the highest kaolinite concentration. Thus, the relative ratio of SS to EPS concentrations played a critical role in determining floc morphology and flocculation potential. According to earlier studies on polymer-induced flocculation (Fleer et al., 1993; Gregory & Barany, 2011; Logan, 2012), EPS molecules could promote bridging flocculation, with developing large and fluffy flocs with polymeric bridges among kaolinite particles. However, at a high SS/EPS ratio (e.g., $2.0\ \text{g/L}$ kaolinite dose concentration), bridging flocculation could reduce and build rather small and dense flocs because EPS molecules could shrink and attach tightly on kaolinite surfaces by adsorption and polymeric chain reformation. Increasing kaolinite concentration and ionic strength could result in more compact polymeric chain structures on kaolinite surfaces (Gregory & Barany, 2011). It is also important to note that both the filtered and unfiltered river water samples had similar results (blue and red lines and symbols in Figure 3). Thus, it is likely that algal cells or biomass contained in the

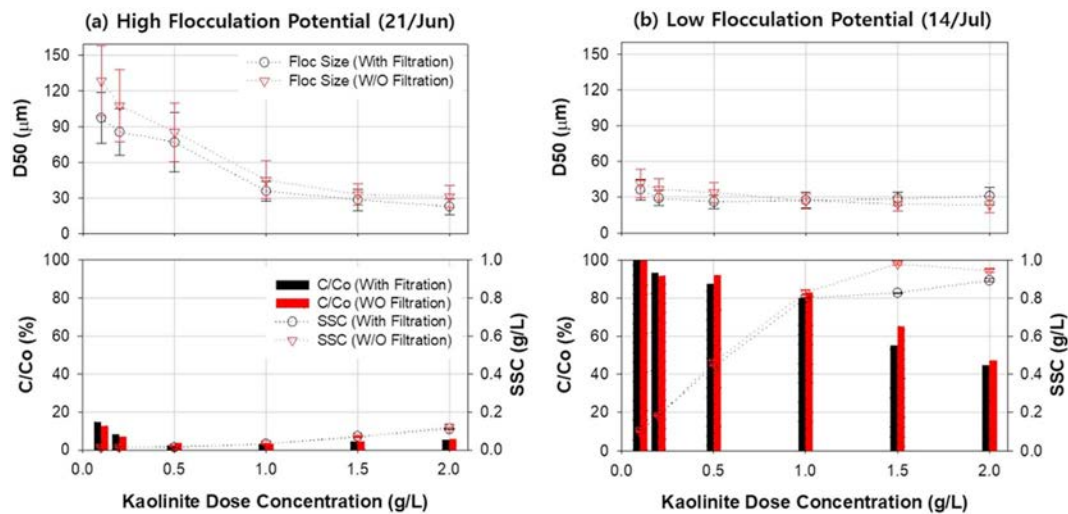


Figure 3. Typical results from the flocculation potential tests with (a) high flocculation potential and (b) low flocculation potential. The top panel of each figure shows the average floc diameters of the circle of equal area (D50), and the bottom panel shows the normalized ratios of the residual solid concentration (C/Co) and the suspended solid concentration (SSC). The experimental indices (D50 and C/Co) were measured in the flocculation potential tests with the kaolinite-dosed river water samples.

unfiltered river water samples might not have had enough EPS in their surface layers to further enhance the flocculation potential.

The flocculation potential of each jar test experiment highly depended on the weather and hydrological conditions. Flocculation prevailed over stabilization during the algae bloom, and vice versa after high rainfall and discharge. The jar test results from samples collected during algae blooms (Figure 3a) presented high D50, up to 128.7 and 97.5 μm , and low C/Co, as low as 14.7 and 12.7%, for the filtered and unfiltered samples, respectively, indicating high flocculation potential. Large flocs (i.e., high D50) have a higher settling velocity and lower residual solid concentration (i.e., low C/Co) than smaller flocs. In contrast, the jar test results after high rainfall and discharge (Figure 3b) displayed D50 of less than 41.7 μm and C/Co of higher than 44.7%, up to 100 %, indicating low extents of flocculation and sedimentation, for both the filtered and unfiltered water samples.

The OM composition that affects the flocculation potential could be identified with the LC-OCD, as it consists of different size fractions of biopolymers, HS, building blocks, and LMW neutrals and acids (denoted by A, B, C, and D, respectively, in Figure 4). The river water samples during the algae bloom period showed a higher biopolymer peak on the OCD chromatogram (peak A of the green line on the top panel of Figure 4), compared to those during high rainfall. No or little peak of biopolymers on the UVD chromatogram (peak A of the green line on the bottom panel of Figure 4) indicated that they are polysaccharides without UV-susceptible aromatic structures. In contrast, the samples after high rainfall and discharge (Figure 3b) were characterized by the enrichment of HS (peak B of the blue line in Figure 4). Therefore, the OM composition, driven by the weather and hydrological condition, tended to facilitate either flocculation or stabilization of SS in the river water. The seasonal dynamics of and the interactions between the OM composition and the flocculation potential in the river water will be discussed in depth in the sections below.

3.2. Seasonal Dynamics of the OM Composition

The relative abundances of the biopolymers, HS, building blocks, LMW acids, and neutrals were 9.3%, 48.2%, 25.7%, and 16.9%, on average, in the river water samples, respectively, throughout the year. The biopolymers and HS were the size fractions that were highly variable in different seasons, whereas the building blocks and the LMW compounds were the fractions remaining stable (Figure 2c). In particular, the HS concentration varied from 1.5 mg/L TOC during dry seasons to about 2.7 mg/L right after high rainfall and discharges (e.g., 14th July, 20th September, and 30th September). High rainfall and discharge seem to lead to the transportation of a large amount of HS from the catchment areas into the river water. The biopolymer

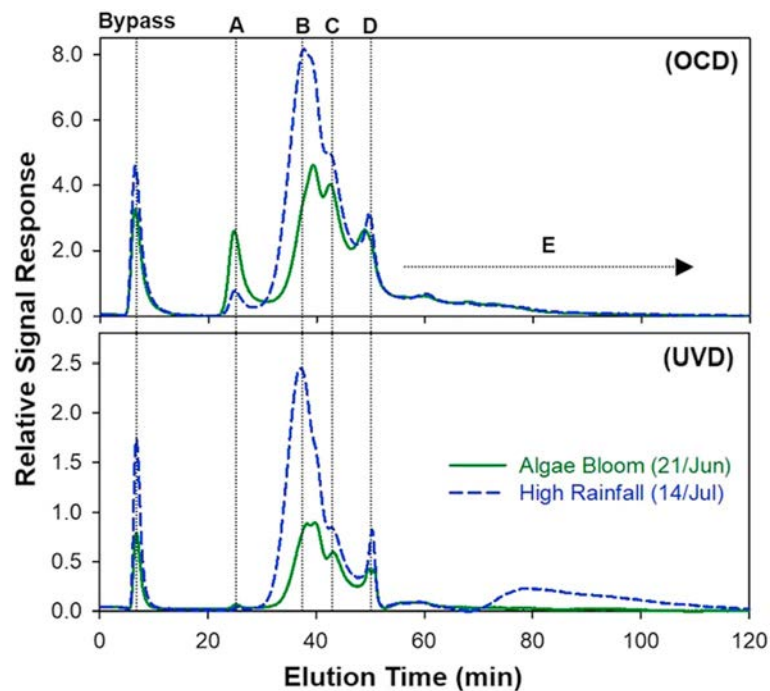


Figure 4. Chromatograms measured by the (top) organic carbon detection (OCD) and (bottom) ultraviolet detection (UVD) devices. Peaks A, B, C, D, and E indicate biopolymers, humic substances, building blocks, low molecular weight organic acids, and neutrals, respectively.

concentration was high in spring and during algae blooms, but decreased after heavy rainfall and discharges (Figures 2b and 2c). Results from the statistical analysis revealed that the seasonal variation of biopolymers and humics concentrations were statistically significant between the two weather conditions after high rainfall and during algae bloom, see Figure 5. The seasonal variation of building blocks was less significant as of biopolymers and humics. In contrast, low MW acids and neutrals had a high *P* value, thus indicating no significant seasonal variation. The respective mean concentrations and standard deviations of biopolymers, humic substances, building blocks, low molecular weight organic acids and neutrals were 0.19 ± 0.02 , 2.66 ± 0.56 , 0.80 ± 0.12 , and 0.58 ± 0.07 mg organic carbon per liter (mgOC/L) after high rainfall and discharge, and 0.41 ± 0.09 , 1.56 ± 0.21 , 1.02 ± 0.11 , and 0.61 ± 0.10 mgOC/L during algae bloom.

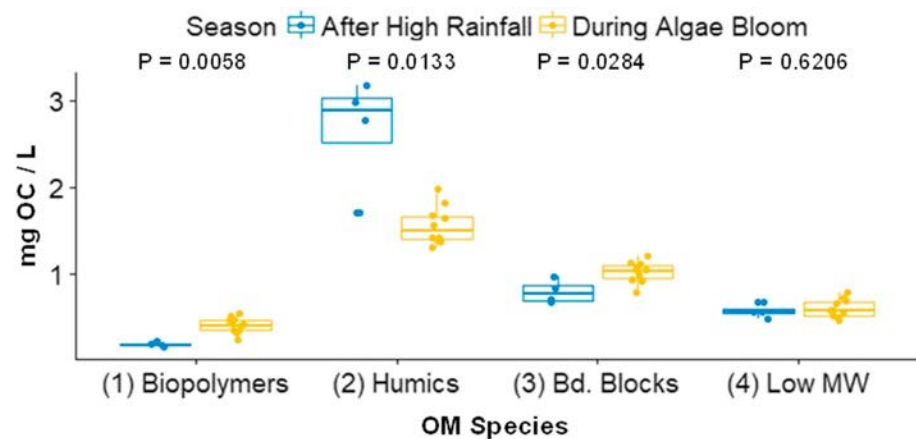


Figure 5. Box plots of organic carbon concentrations (mgOC/L) of the organic matter species (i.e., biopolymers, humics, building blocks, and low molecular weight acids and neutrals), which demonstrate statistical significance of the seasonal variation, during algae bloom and after high rainfall. The *P* values also indicate statistical significance of the seasonal variation.

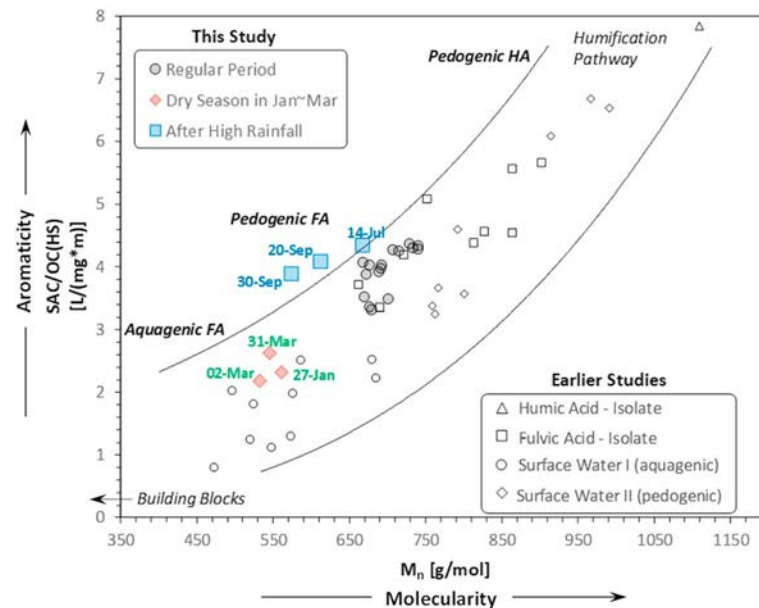
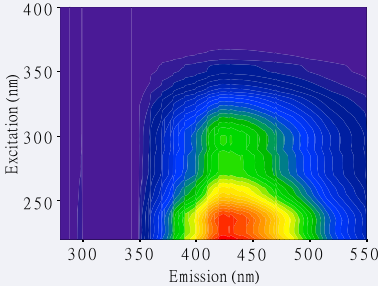
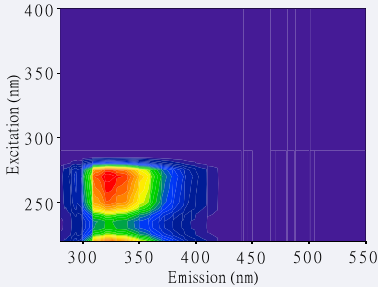
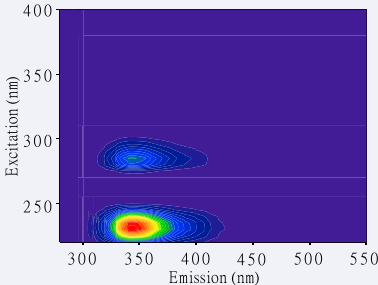


Figure 6. Humic substances (HS) diagram. M_n on the x axis is the nominal average molecular weight, indicating the molecularity of HS compounds, and SAC/OC on the y axis represents the spectral absorption coefficient/organic carbon ratio, indicating the aromaticity. The gray circles, the red diamonds, and the blue squares represent measurements from the regular period, the dry season and after high rainfall in the rainy season, respectively (Modified from Huber et al. (2011)).

The so-called HS diagram can further categorize HS into three subgroups, depending on the molecularity and the aromaticity (i.e., x and y axes in Figure 6; M. Chen et al., 2016; Huber et al., 2011). The three HS subgroups included the aquagenic fulvic acids (FA), the pedogenic FA, and the pedogenic humic acids (HA). Aquagenic FA are characterized by low, pedogenic FA by intermediate, and pedogenic HA by high molecularity and aromaticity (Figure 6). According to Huber and coworkers (Huber et al., 2011), aquagenic FA are usually abundant in stagnant lakes, as they are produced in situ by microbial activity rather than being transported from the catchment areas. Pedogenic FA, however, are discharged by runoff from the catchment areas into a river during high rainfall events. Pedogenic FA are relatively fresh humic substances and often found in small rivers and creeks whose catchment areas have steep slopes. On the other hand, pedogenic HA are also enriched by runoff from the catchment areas, like pedogenic FA, but they are abundant in brown tannin-rich water rivers whose catchment areas are swamps or bogs.

The HS of our river water samples were mostly pedogenic FA throughout the year (Figure 6), probably because the steep slopes of the Nakdong catchment areas facilitated the discharge of fresh FA rather than aging HA. However, the HS diagram also shows some exceptions with respect to the hydrological and anthropogenic stressors. The HS during the dry season (winter to early spring) were characterized as aquagenic FA (marked by the red diamonds in Figure 6, measured on 27 January, 2 March, and 31 March). The weir seemed to increase microbial activity in the lacustrine environment by elongating water retention time, thereby promoting aquagenic FA production. The aquagenic FA were then replaced by pedogenic FA, which discharged from the catchment areas after the rainfall and discharges in the spring. Subsequently, the HS composition underwent significant changes during the summer rainy season. The data points corresponding to 14 July, 20 September, and 30 September, right after high rainfall and discharges, sit near the upper margin of the humification pathway of the HS diagram (marked by the blue squares in Figure 6), indicating higher aromaticity. These data points correspond to the high peaks in HS concentrations during the rainy seasons (see also Figures 2b and 2c). The highly aromatic pedogenic FA might have been transported from the catchment areas into the river, thus replacing the aquagenic FA. Overall, the hydrological processes and associated weir operational scheme facilitated changes in the study site from a riverine to a more lacustrine status, and vice versa, ultimately determining the OM composition.

Table 1
Characteristics of the Fluorescence Excitation-Emission Matrices (EEM) Peaks in this study

Comp.	Peak ($\lambda_{ex}/\lambda_{em}$)	FEEM responses	Description
C1	230/430		Humic-like component; fulvic acid; terrestrial (i.e., pedogenic) organic matter; high molecular weight and aromatic compounds discharged from wetlands and forested environments
C2	270(≤ 225)/320		Tyrosine-like component; autochthonous (i.e., aquagenic) organic matter; amino acids, free or bound in proteins, associated with aquatic biological activities
C3	$\leq 225(280)/345$		Tryptophan-like component; autochthonous (i.e., aquagenic) organic matter; amino acids, free or bound in proteins, associated with aquatic biological activities

Note. Values in brackets represent the secondary peak. Information about the EEM peaks was obtained from earlier studies (Coble, 1996; Coble et al., 1998; Fellman et al., 2010; B. J. Lee et al., 2017; Murphy et al., 2011; Yang, Hur, et al., 2015; Y. Zhang et al., 2010).

The EEM-PARAFAC results supported the findings from the LC-OCD. The EEM-PARAFAC showed that fluorescent OM can be described by a three-component model, consisting of C1, C2, and C3 components, which have their excitation/emission maxima at 230/430 nm, 270(≤ 225)/320 nm, and $\leq 225/345$ nm, respectively (Table 1). According to previous studies (Coble, 1996; Coble et al., 1998; Fellman et al., 2010; B. J. Lee et al., 2017; Murphy et al., 2011; Yang, Hur, et al., 2015; Y. Zhang et al., 2010), the C1, C2, and C3 components can be assigned to humic-like, tyrosine-like, and tryptophan-like fluorescent OM, respectively. The humic-like C1 component could be pedogenic in origin, transported from the catchment areas. In contrast, the tyrosine-like C2 and the tryptophan-like C3 components could be aquagenic or autochthonous in origin, produced by in situ microbial activity. Thus, C1 could be analogous to pedogenic FA, whereas C2 and C3 could be analogous to aquagenic FA, shown in the HS diagram (Figure 6).

The EEM-PARAFAC results also revealed seasonal variation of the OM composition, similarly to the LC-OCD results. For example, the C2 and C3 components were enriched in the OM composition on 27 January, 2 Mar, and 30 Mar (winter dry season), concurring with the presence of the highly aquagenic FA on the HS diagram (Figures 2d and 7). As discussed in the earlier section, less discharges and long water retention time during the dry season results in a more lacustrine environment. This causes an increase in microbial activity and, thus, the production of aquagenic FA. Rainfall and discharge events in spring resulted in the depletion of the protein-like components (i.e., C2 and C3), but enriched C1. Afterward, the summer rainy season caused a sudden increase of the C1 component (Figure 2d), which coincided with the sudden increase of the HS concentration, detected by LC-OCD (Figure 2c). The triangular diagram

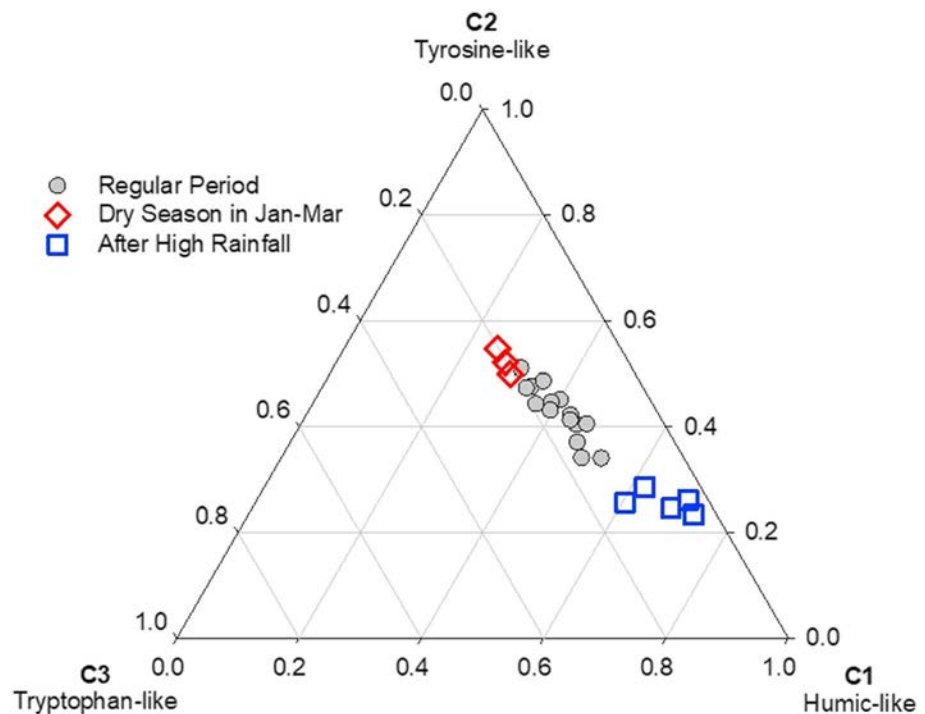


Figure 7. Triangular diagram of the C1, C2, and C3 organic matter fractions, quantified by the fluorescence excitation-emission matrix spectroscopy coupled with parallel factor analysis (EEM-PARAFAC). The gray circles, the red diamonds, and the blue squares represent measurements from the regular period, the dry season, and after high rainfall in the rainy season, respectively.

with the C1, C2, and C3 components (Figure 7) shows the seasonal shifts of the OM composition in a similar way to the HS diagram (Figure 6). The OM components in the winter dry season lie on the upper middle part of the triangular diagram with an abundance of the protein-like components (i.e., C2 and C3) (red diamonds in Figure 7), whereas those during the summer rainy season sit on the lower right side with an enrichment of C1 (blue squares in Figure 7). The former and the latter cases indicate the two extremes of the riverine and lacustrine conditions (i.e., the aquagenic and pedogenic OM characteristics), respectively.

3.3. Seasonal Dynamics of Flocculation Potential

The flocculation potential (i.e., D50 and C/Co), obtained from all the jar tests on samples collected throughout the year, shows apparent seasonal variations (Figure 8). In spring (30 March to 15 June), C/Co generally remained at low levels. Such a low C/Co indicates high flocculation potential. After the spring period, the flocculation potential further increased on 21 and 30 June, indicated by a rise of D50 and a drop of C/Co, which corresponded to the peak season for the BGA number (i.e., algae bloom). Another peak in the flocculation potential (i.e., high D50 and low C/Co) was found on 4 and 11 August during the second algae bloom. Such high flocculation potential concurred with a high biopolymer concentration during the dry seasons, in the winter, and early spring and summer (Figure 2b).

The high flocculation potential, associated with algae blooms, did not persist for the entire summer. A sudden decrease of the flocculation potential (i.e., a drop of D50 and a peak of C/Co) occurred right after high rainfall and discharges on 23 and 29 July and 20 and 30 September (Figure 8). The abrupt decline of the flocculation potential corresponded to the data points with the high aromaticity on the HS diagram and the high C1 component on the triangular OM diagram (see blue squares in Figures 6 and 7). It is obvious that the flocculation potential of the river water samples correlated with the OM composition.

3.4. Redundancy Analysis on Multivariables and Descriptors

The flocculation potential descriptors (i.e. D50 and C/Co) and the OM compositional, hydrological and water quality variables were statistically evaluated using RDA, where the respective RDA axes account for

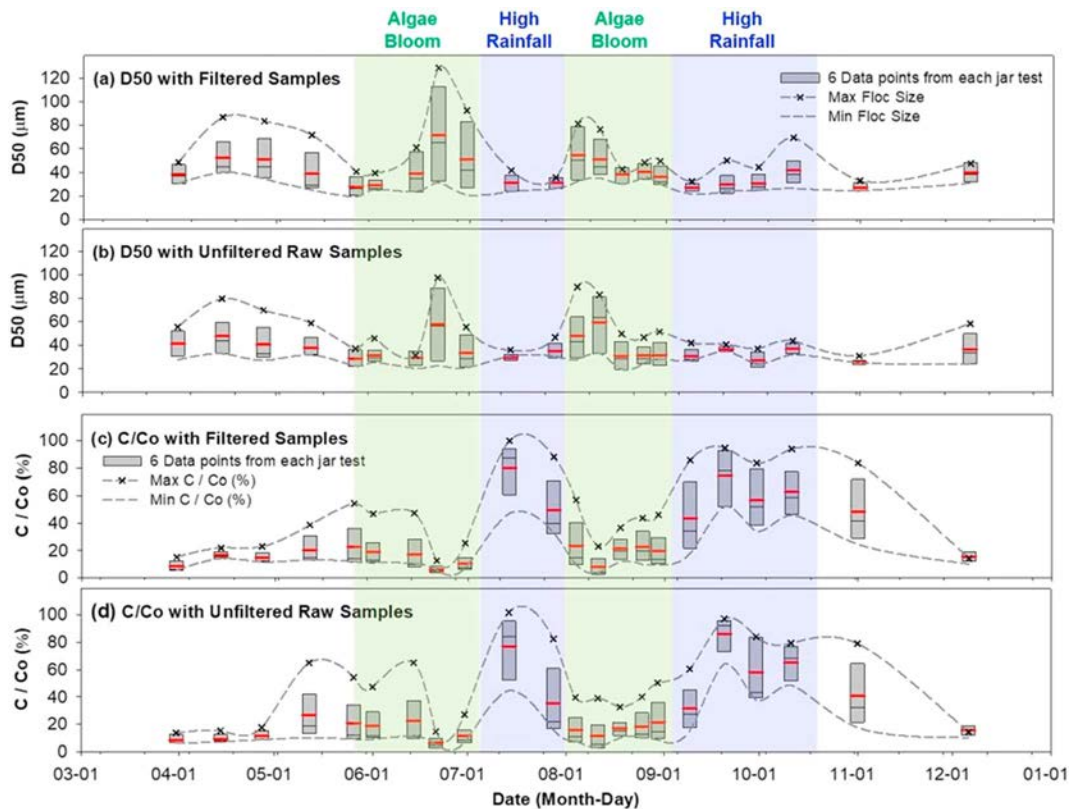


Figure 8. Seasonal variations of the flocculation potential of the river water samples. The respective panels represent the yearly box plots of (a) D50 (average floc diameter of the circle of equal area) measured in the jar test experiments with the filtered water samples, (b) D50 with the unfiltered raw water samples, (c) C/Co (the normalized ratios of the residual solid concentration) with the filtered water samples, (d) C/Co with the unfiltered raw water samples. The respective black and red lines in a box plot indicate the median and mean values of the measured flocculation indices in a jar test.

41.8% and 2.2% of the variance (Figure 9a). The RDA1 axis strongly correlates with the variables from both riverine and lacustrine water. The typical riverine variables, such as water discharge, humics, humic-like pedogenic component (C1), and total phosphorus (TP) concentration, were positively correlated with RDA1. In contrast, the negative loadings on RDA1 were found for the lacustrine variables, such as electrical conductivity (EC) and protein-like components (i.e., C2 and C3). Although the RDA2 axis does not have as strong a correlation as RDA1 with the variables, it showed a positive correlation with dissolved oxygen (DO), but a negative one with temperature. It can be interpreted from the variables' locations that RDA2 is associated with biological activity, especially with oxygen-depleting microorganisms that feed on algal biomass during high temperature.

Concerning the OM composition, C1 and humics have strong positive correlations with RDA1, projecting themselves on the first quadrant along with water discharge and, hence, indicating their abundance in a riverine condition. However, C2 and C3 are negatively correlated with RDA1, indicating their strong linkages with a lacustrine condition (i.e., less discharge and higher EC). Building blocks and LMW acids and neutrals, which remained relatively constant throughout the year, show negative correlations with RDA2, probably as they were under the influence of the oxygen-depleting microbial activity. The flocculation potential descriptors of C/Co and D50 show dependence on RDA1 and RDA2, respectively. For instance, C/Co has a highly positive loading on RDA1, projecting along with the riverine variables, such as C1, humics, and water discharge. Unlike C/Co, D50 is projected negatively along RDA2, suggesting a weak association of this descriptor with the microbial activity.

The seasonal variations, with respect to hydrological and biogeochemical conditions, as well as stabilization/flocculation-favorable conditions, are well discriminated in the RDA biplot of the descriptors and individuals (Figure 9b). The individuals in the stabilization-favorable condition (shaded with blue

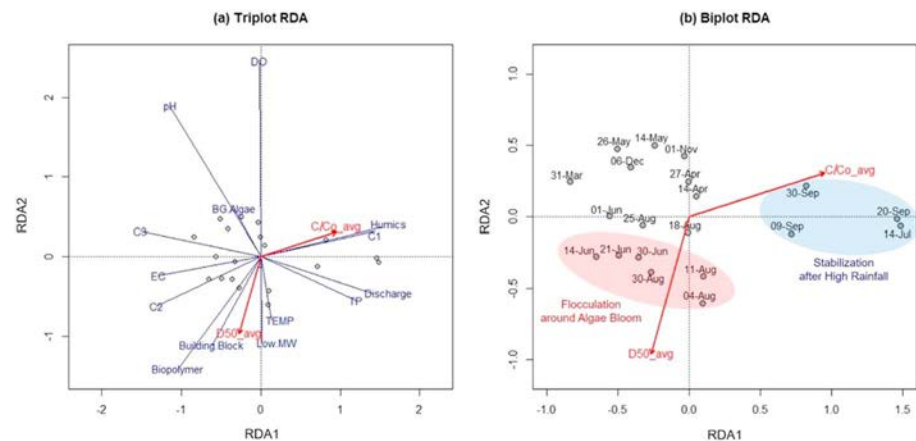


Figure 9. Graphical representation of redundancy analysis (RDA). (a) Loadings of the hydrological and water quality variables, the flocculation potential descriptors, and the individuals with the RDA1 and RDA2 axes. (b) Loadings of the flocculation potential descriptors and the individuals (i.e., measurement date) with RDA1 and RDA2. The respective variables of BG Algae, Discharge, DO, pH, TEMP, and TP represent blue-green algae number concentration, water discharge rate, dissolved oxygen concentration, temperature, and total phosphorus concentration. The humic-, the tyrosine-like, and the tryptophan-like fractions measured with EEM-PARAFAC are denoted as C1, C2, and C3. The concentrations of biopolymers, humic substances, building block, and low molecular weight compounds measured with LC-OCD are denoted as Biopolymer, Humics, Building Block, and Low MW, respectively. D50_avg and C/Co_avg, as the flocculation potential descriptors, indicate the averaged values of all the D50 and C/Co values measured in the jar test experiment.

color in Figure 9b) are projected on or near the RDA1 axis, along with high C/Co, discharge, C1, and humics. In contrast, the individuals in the flocculation-favorable condition during algae bloom (shaded with red color in Figure 9b) are loaded on the third quadrant, along with high D50, algae, building blocks and biopolymers. The RDA results demonstrate the roles that weather, along with hydrological, biochemical, and anthropogenic stressors, play in changing the OM composition and flocculation potential of river water, which supports the results and discussion of Larsen and coworkers (Larsen et al., 2010).

3.5. Conceptualization of OM and Suspended Sediment Dynamics in River Water

The river with the constructed weirs could be riverine or lacustrine, depending on the season and weir operation, which consequently changes the OM composition and flocculation potential throughout the year. For example, the weir operation scheme that is intended to secure water resources during the dry season likely creates a more lacustrine environment and promotes microbial production of aquagenic OM. Our previous OM analyses revealed the prevalence of aquagenic OM during the dry season, which tended to increase the flocculation potential of the river water (see the earlier sections 3.2 and 3.3).

Persistence of warm and sunny weather in summer further promotes primary production and microbial activity. In this study, a high flocculation potential, facilitated by high biopolymer concentration, occurred during algae blooms (i.e., during peak primary production). This observation is consistent with earlier reports that EPS formation and EPS-mediated flocculation occur during algae bloom (Engel et al., 2004; Fettweis et al., 2014; Fettweis & Lee, 2017; Jackson, 1995; W. T. B. van der Lee, 2000; Sahoo et al., 2013). Together with EPS as sticky binders, biomass and SS aggregate to large biomineral flocs and eventually will settle on the river bed (Figure 10b; Droppo, 2001; Fettweis & Lee, 2017; Larsen, Harvey, & Crimaldi, 2009; Larsen, Harvey, Noe, et al., 2009; Maggi, 2013; Maggi & Tang, 2015; Zimmermann-Timm, 2002). Dark-colored mucky sediments, which are often found in highly eutrophic lakes, comprise a typical example of a deposition that originates from EPS-mediated biomineral flocculation (Ali et al., 1988).

The flocculation-favorable condition, however, did not last the entire summer and switched toward a stabilization-favorable condition during the rainfall events in summer (Figure 10c). High rainfall and discharges from the catchment areas transported a large amount of HS (i.e., pedogenic FA) into the river water. The abundant HS in the river water could dominate over EPS with regard to adsorption on colloidal particles (e.g., kaolinite particles in this study). HS can quickly attach to particle surfaces because of their high reactivity and mobility. Adsorbed HS on colloidal particles operate to hinder flocculation, because

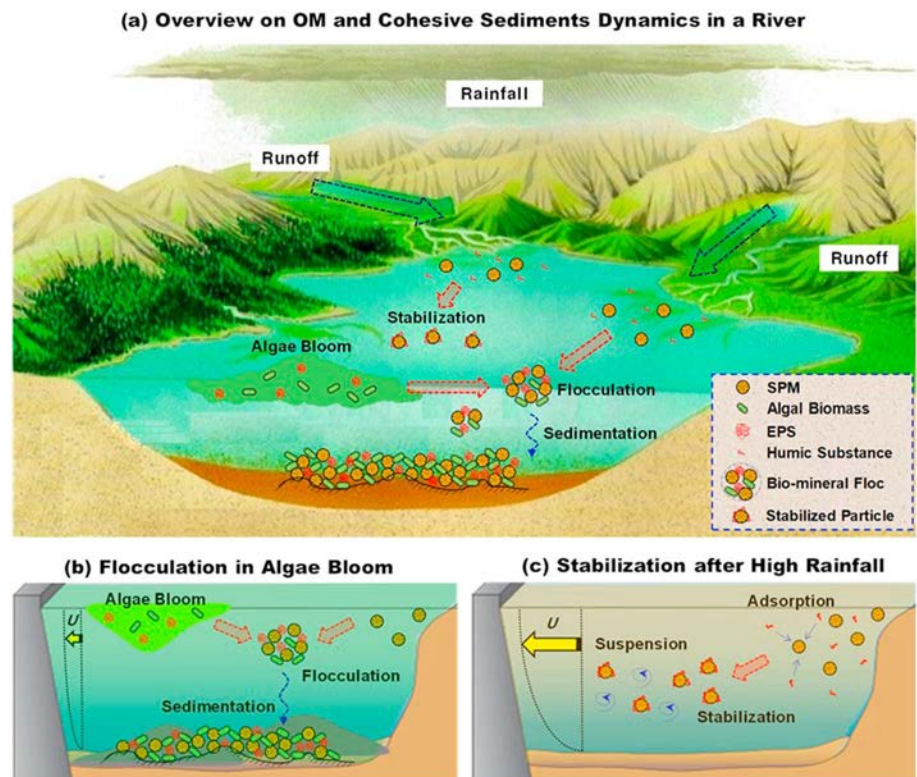


Figure 10. Schematic diagram of the conceptual model, describing the fate and transport of organic matter and suspended sediment in a river or lake. The respective figures represent (a) the organic matter and suspended sediment dynamics, (b) the aquagenic, flocculation-favorable condition in the dry season, and (c) the pedogenic, stabilization-favorable condition after high rainfall in the rainy season.

they modify the surface characteristics in a way to increase the electrostatic repulsion and steric stabilization (Fleer et al., 1993; Jekel, 1986; Kretzschmar et al., 1998; Logan, 2012; Wilkinson et al., 1997). The abundant HS during the rainy season, accompanied by high flow and turbulence, enhances particle stabilization and resuspension of cohesive (or biomineral) sediments, and increases the turbidity of the water.

4. Conclusions

The OM composition of the river water was found to be dynamic in the river with the weirs, under different weather, hydrological, biochemical, and anthropogenic conditions, and appeared to play a critical role in determining the flocculation potential of the river water. The findings of this research are summarized in the paragraphs below.

1. The LC-OCD and the EEM-PARAFAC revealed that the OM composition of the river water became aquagenic with the abundance of biopolymers and protein-like OM components during the dry seasons, but more pedogenic with the dominance of HS during the rainy seasons.
2. The flocculation potential was found to depend on the OM composition, as it increased with a higher fraction of aquagenic OM but decreased with the presence of pedogenic components. In particular, the flocculation potential depended on the relative proportion of EPS and HS in the OM pool. The flocculation potential sharply increased during algae bloom due to high primary production and EPS formation, whereas it decreased during high rainfall and discharge because of the HS transport into the river water that favors stabilization.
3. The multivariate data analysis demonstrated that the OM composition and flocculation potential strongly correlated with the riverine and lacustrine variables of the river water. The riverine variables were identified to be water discharge, phosphorus concentration and pedogenic OM species (e.g., humic-like C1, HS), and the lacustrine variables were electrical conductivity and aquagenic OM species (e.g., protein-like C2 and C3, and biopolymers).

Hydraulics and hydrological studies on water resources management have been mainly focusing on the economic and engineering perspective. The findings of this study indicate that biochemistry, in association with weather, hydrological, and anthropogenic conditions, should be included in water resources management. Based on the findings of this study, a specific biochemical condition during algae bloom can enhance biologically mediated flocculation, sedimentation, and deposition, and eventually will result in hypoxia near the river bed and degrade the water and sediment quality. On the other hand, a biochemical condition with abundant pedogenic HS during rainy seasons could enhance particle stabilization, and hence will result in highly turbid river water that also degrades the water quality. No doubt, multidisciplinary approaches are needed to understand OM and SS dynamics, and to solve various water and sediment quality issues. This study could serve as a first step to integrate different academic disciplines to improve the understanding of aquatic processes and the management of water and sediment quality in water resources.

Nomenclature

BGA	Blue-green algae
C/Co	Normalized ratios of the residual solids concentration against the total concentration in the water column
DO	Dissolved oxygen
DOC	Dissolved organic carbon
D50	Average floc diameter of the circle of equal area (Heywood diameter).
EC	Electrical conductivity
EPS	Extracellular polymeric substances
FA	Fulvic acids
EEM-PARAFAC	Excitation-emission matrix spectroscopy coupled with parallel factor analysis
HA	Humic acids
HS	Humic substances
LC-OCD	Liquid chromatography-organic carbon detection
LMW	Low molecular weight
MW	Molecular weight
OCD	Organic carbon detector
OM	Organic matter
RDA	Redundancy analysis
SCFA	Surfactant free cellulose acetate
SS	Suspended sediment
SSC	Suspended sediment concentration
SUVA	Specific ultra-violet absorbance
TOC	Total organic carbon
TP	Total phosphorus
UVD	Ultraviolet detector
XG	Xanthan gum

Acknowledgments

This research was supported by the Basic Science Research Program through the National Research Foundation of Korea (NRF), funded by the Ministry of Education (NRF-2017R1D1A3B03035269). Data reported in this paper can be accessed in the figshare data repository (https://figshare.com/articles/Experimental_and_Monitoring_Data_on_Organic_Matter_Composition_and_Flocculation_Potential_in_Nakdong_River_Korea/7378364) (B. J. Lee, 2018).

References

- Ali, A., Reddy, K., & DeBusk, W. (1988). Seasonal changes in sediment and water chemistry of a subtropical shallow eutrophic lake. *Hydrobiologia*, *159*, 159–167.
- APHA (1998). *Standard Methods for the Examination of Water and Wastewater*, 20th Edition. Washington, DC, USA: American Public Health Association.
- Bade, D. L., Carpenter, S. R., Cole, J. J., Pace, M. L., Kritzberg, E., van de Bogert, M. C., et al. (2007). Sources and fates of dissolved organic carbon in lakes as determined by whole-lake carbon isotope additions. *Biogeochemistry*, *84*(2), 115–129. <https://doi.org/10.1007/s10533-006-9013-y>
- Bainbridge, Z., Wolanski, E., Alvarez-Romero, J. G., Lewis, S. E., & Brodie, J. E. (2012). Fine sediment and nutrient dynamics related to particle size and floc formation in a Burdekin River flood plume, Australia. *Marine Pollution Bulletin*, *65*(4-9), 236–248. <https://doi.org/10.1016/j.marpolbul.2012.01.043>
- Buttigieg, P. L., & Ramette, A. (2014). A guide to statistical analysis in microbial ecology: A community-focused, living review of multi-variate data analyses. *FEMS Microbiology Ecology*, *90*(3), 543–550. <https://doi.org/10.1111/1574-6941.12437>
- Capuzzo, E., Stephens, D., Silva, T., Barry, J., & Forster, R. M. (2015). Decrease in water clarity of the southern and central North Sea during the 20th century. *Global Change Biology*, *21*(6), 2206–2214. <https://doi.org/10.1111/gcb.12854>

- Chen, M., He, W., Choi, I., & Hur, J. (2016). Tracking the monthly changes of dissolved organic matter composition in a newly constructed reservoir and its tributaries during the initial impounding period. *Environmental Science and Pollution Research*, 23(2), 1274–1283. <https://doi.org/10.1007/s11356-015-5350-5>
- Chen, M. S., Wartel, S., & Temmerman, S. (2005). Seasonal variation of floc characteristics on tidal flats, the Scheldt estuary. *Hydrobiologia*, 540(1-3), 181–195. <https://doi.org/10.1007/s10750-004-7143-6>
- Coble, P. G. (1996). Characterization of marine and terrestrial DOM in seawater using excitation–emission matrix spectroscopy. *Marine Chemistry*, 51(4), 325–346. [https://doi.org/10.1016/0304-4203\(95\)00062-3](https://doi.org/10.1016/0304-4203(95)00062-3)
- Coble, P. G., del Castillo, C. E., & Avril, B. (1998). Distribution and optical properties of CDOM in the Arabian Sea during the 1995 southwest monsoon. *Deep-Sea Research Part II*, 45, 2195–2223.
- Droppo, I. G. (2001). Rethinking what constitutes suspended sediment. *Hydrological Processes*, 15(9), 1551–1564. <https://doi.org/10.1002/hyp.228>
- Engel, A., Thoms, S., Riebesell, U., Rochelle-Newall, E., & Zondervan, I. (2004). Polysaccharide aggregation as a potential sink of marine dissolved organic carbon. *Nature*, 428(6986), 929–932. <https://doi.org/10.1038/nature02453>
- Fellman, J., Hood, E., & Spencer, G. (2010). Fluorescence spectroscopy opens new windows into dissolved organic matter dynamics in freshwater ecosystems: A review. *Limnology and Oceanography*, 55(6), 2452–2462. <https://doi.org/10.4319/lo.2010.55.6.2452>
- Fettweis, M., & Baeye, M. (2015). Seasonal variation in concentration, size and settling velocity of muddy marine flocs in the benthic boundary layer. *Journal of Geophysical Research: Oceans*, 120, 5648–5667. <https://doi.org/10.1002/2014JC010644>
- Fettweis, M., Baeye, M., van der Zande, D., van den Eynde, D., & Lee, B. J. (2014). Seasonality of floc strength in the southern North Sea. *Journal of Geophysical Research: Oceans*, 119, 1911–1926. <https://doi.org/10.1002/2013JC009750>
- Fettweis, M., & Lee, B. (2017). Spatial and seasonal variation of biomineral suspended particulate matter properties in high-turbid near-shore and low-turbid offshore zones. *Water*, 9(9), 694. <https://doi.org/10.3390/w9090694>
- Fleer, G., Cohen Stuart, M., Scheutjens, J., & Cosgrove, T. (1993). *Polymers at interfaces*. London, UK: Chapman & Hall.
- Furukawa, Y., Reed, A. H., & Zhang, G. (2014). Effect of organic matter on estuarine flocculation: A laboratory study using montmorillonite, humic acid, xanthan gum, guar gum and natural estuarine flocs. *Geochemical Transactions*, 15(1), 1–9. <https://doi.org/10.1186/1467-4866-15-1>
- Gorczyca, B., & Ganczarczyk, J. (1996). Image analysis of alum coagulated mineral suspensions. *Environmental Technology*, 17(12), 1361–1369. <https://doi.org/10.1080/09593331708616505>
- Gregory, J., & Barany, S. (2011). Adsorption and flocculation by polymers and polymer mixtures. *Advances in Colloid and Interface Science*, 169(1), 1–12. <https://doi.org/10.1016/j.cis.2011.06.004>
- Huber, S., Balz, A., Abert, M., & Pronk, W. (2011). Characterisation of aquatic humic and non-humic matter with size-exclusion chromatography—organic carbon detection—organic nitrogen detection (LC-OCD-OND). *Water Research*, 45(2), 879–885. <https://doi.org/10.1016/j.watres.2010.09.023>
- Huber, S., & Frimmel, F. (1994). Direct gel chromatographic characterization and quantification of marine dissolved organic carbon using high-sensitivity DOC detection. *Environmental Science and Technology*, 28(6), 1194–1197. <https://doi.org/10.1021/es00055a035>
- Hudson, N., Baker, A., & Reynolds, D. (2007). Fluorescence analysis of dissolved organic matter in natural, waste and polluted waters—A review. *River Research and Applications*, 23(6), 631–649. <https://doi.org/10.1002/rra.1005>
- Hur, J., & Cho, J. (2012). Prediction of BOD, COD, and total nitrogen concentrations in a typical urban river using a fluorescence excitation–emission matrix with PARAFAC and UV absorption indices. *Sensors-Basel*, 12(1), 972–986. <https://doi.org/10.3390/s120100972>
- Jackson, G. (1995). Comparing observed changes in particle size spectra with those predicted using coagulation theory. *Deep Sea Research, Part II*, 42(1), 159–184. [https://doi.org/10.1016/0967-0645\(95\)00010-N](https://doi.org/10.1016/0967-0645(95)00010-N)
- Jekel, M. R. (1986). The stabilization of dispersed mineral particles by adsorption of humic substances. *Water Research*, 20(12), 1543–1554. [https://doi.org/10.1016/0043-1354\(86\)90119-3](https://doi.org/10.1016/0043-1354(86)90119-3)
- Joung, S., Kim, C., Ahn, C., Jang, K., Boo, S., & Oh, H. (2006). Simple method for a cell count of the colonial cyanobacterium, *Microcystis* sp. *Journal of Microbiology*, 44(5), 562–565.
- Jun, K., & Kim, J. (2011). The four major rivers restoration project: Impacts on river flows. *KSCSE Journal of Civil Engineering*, 15(2), 217–224. <https://doi.org/10.1007/s12205-011-0002-x>
- Kondolf, G. M., Gao, Y., Annandale, G. W., Morris, G. L., Jiang, E., Zhang, J., et al. (2014). Sustainable sediment management in reservoirs and regulate drivers: Experiences from five continents. *Earth's Future*, 2, 256–280. <https://doi.org/10.1002/2013EF000184>
- Kondolf, G. M., & Wilcock, P. R. (1996). The flushing flow problem: Defining and evaluating objectives. *Water Resources Research*, 32(8), 2589–2599. <https://doi.org/10.1029/96WR00898>
- Korea Ministry of Environment (2016). *Official water quality test methods (in Korean)*. Seoul, Korea: Ministry of Environment.
- Kretzschmar, R., Holthoff, H., & Sticher, H. (1998). Influence of pH and humic acid on coagulation kinetics of kaolinite: A dynamic light scattering study. *Journal of Colloid and Interface Science*, 202(1), 95–103. <https://doi.org/10.1006/jcis.1998.5440>
- Kritzberg, E. S., Cole, J. J., Pace, M. L., Graneli, W., & Bade, D. L. (2004). Autochthonous versus allochthonous carbon sources of bacteria: Results from whole-lake ¹³C addition experiments. *Limnology and Oceanography*, 49(2), 588–596. <https://doi.org/10.4319/lo.2004.49.2.0588>
- Labille, J., Thomas, F., Milas, M., & Vanhaverbeke, C. (2005). Flocculation of colloidal clay by bacterial polysaccharides: Effect of macromolecule charge and structure. *Journal of Colloid and Interface Science*, 284(1), 149–156. <https://doi.org/10.1016/j.jcis.2004.10.001>
- Lah, T., Park, Y., & Cho, Y. (2015). The four major rivers restoration project of South Korea: An assessment of its process, program, and political dimensions. *Journal of Environment & Development*, 24(4), 375–394. <https://doi.org/10.1177/1070496515598611>
- Larsen, L. G., Aiken, G. R., Harvey, J. W., Noe, G. B., & Crimaldi, J. P. (2010). Using fluorescence spectroscopy to trace seasonal DOM dynamics, disturbance effects, and hydrologic transport in the Florida Everglades. *Journal of Geophysical Research*, 115, G03001. <https://doi.org/10.1029/2009JG001140>
- Larsen, L. G., Harvey, J. W., & Crimaldi, J. P. (2009). Morphologic and transport properties of natural organic floc. *Water Resources Research*, 45, W01410. <https://doi.org/10.1029/2008WR006990>
- Larsen, L. G., Harvey, J. W., Noe, G. B., & Crimaldi, J. P. (2009). Predicting organic floc transport dynamics in shallow aquatic ecosystems: Insights from the field, the laboratory, and numerical modeling. *Water Resources Research*, 45, W01411. <https://doi.org/10.1029/2008WR007221>
- Lee, B. H., & Jeong, G. H. (2008). Distribution of clay minerals in soils on the northern drainage basin of the Nakdong River. *Journal of the Mineralogical Society of Korea*, 21(4), 349–354.

- Lee, B. J. (2018). Experimental and monitoring data on organic matter composition and flocculation potential in Nakdong River, Korea. Retrieved from https://figshare.com/articles/Experimental_and_Monitoring_Data_on_Organic_Matter_Composition_and_Flocculation_Potential_in_Nakdong_River_Korea/7378364
- Lee, B. J., Fettweis, M., Toorman, E., & Molz, F. J. (2012). Multimodality of a particle size distribution of cohesive suspended particulate matters in a coastal zone. *Journal of Geophysical Research*, *117*, C03014. <https://doi.org/10.1029/2011JC007552>
- Lee, B. J., Hur, J., & Toorman, E. A. (2017). Seasonal variation in flocculation potential of river water: Roles of the organic matter pool. *Water*, *9*(5), 335. <https://doi.org/10.3390/w9050335>
- Lee, B. J., & Schlautman, M. A. (2015). Effects of polymer molecular weight on adsorption and flocculation in aqueous kaolinite suspensions dosed with nonionic polyacrylamides. *Water*, *7*(11), 5896–5909. <https://doi.org/10.3390/w7115896>
- Lee, B. J., Schlautman, M. A., Toorman, E., & Fettweis, M. (2012). Competition between kaolinite flocculation and stabilization in divalent cation solutions dosed with anionic polyacrylamides. *Water Research*, *46*(17), 5696–5706. <https://doi.org/10.1016/j.watres.2012.07.056>
- Legendre, P., & Legendre, L. (1998). *Numerical ecology*, (2nd ed.). Amsterdam: Elsevier.
- Leng, X., Startchev, K., & Buffle, J. (2002). Application of fluorescence correlation spectroscopy: A study of flocculation of rigid rod-like biopolymer (schizophyllan) and colloidal particle. *Journal of Colloid and Interface Science*, *251*(1), 64–72. <https://doi.org/10.1006/jcis.2002.8429>
- Logan, B. (2012). *Environmental transport processes*, (2nd ed.). New York, NY: John Wiley & Sons, Inc. <https://doi.org/10.1002/9781118230107>
- Maggi, F. (2005). Flocculation dynamics of cohesive sediment (PhD Dissertation). The Netherlands: Technische Universiteit Delft.
- Maggi, F. (2009). Biological flocculation of suspended particles in nutrient-rich aqueous ecosystems. *Journal of Hydrology*, *376*(1-2), 116–125. <https://doi.org/10.1016/j.jhydrol.2009.07.040>
- Maggi, F. (2013). The settling velocity of mineral, biomineral, and biological particles and aggregates in water. *Journal of Geophysical Research: Oceans*, *118*, 2118–2132. <https://doi.org/10.1002/jgrc.20086>
- Maggi, F., & Tang, F. H. M. (2015). Analysis of the effect of organic matter content on the architecture and sinking of sediment aggregates. *Marine Geology*, *363*, 102–111. <https://doi.org/10.1016/j.margeo.2015.01.017>
- Mietta, F., Chassagne, C., Manning, A. J., & Winterwerp, J. C. (2009). Influence of shear rate, organic matter content, pH and salinity on mud flocculation. *Ocean Dynamics*, *59*(5), 751–763. <https://doi.org/10.1007/s10236-009-0231-4>
- Mietta, F., Chassagne, C., & Winterwerp, J. (2009). Shear-induced flocculation of a suspension of kaolinite as function of pH and salt concentration. *Journal of Colloid and Interface Science*, *336*(1), 134–141. <https://doi.org/10.1016/j.jcis.2009.03.044>
- Murphy, K. R., Hambly, A., Singh, S., Henderson, R. K., Baker, A., Stuetz, R., & Khan, S. J. (2011). Organic matter fluorescence in municipal water recycling schemes: Toward a unified PARAFAC model. *Environmental Science & Technology*, *45*(7), 2909–2916. <https://doi.org/10.1021/es103015e>
- Oksanen, J., Blanchet, F. G., Friendly, M., Kindt, R., Legendre, P., McGlinn, D., et al. (2019). Package “vegan”: Community ecology package. Retrieved from <https://github.com/vegandevs/vegan>
- Palmer, M. E., Yan, N. D., Paterson, A. M., & Girard, R. E. (2011). Water quality changes in south-central Ontario lakes and the role of local factors in regulating lake response to regional stressors. *Canadian Journal of Fisheries and Aquatic Sciences*, *68*(6), 1038–1050. <https://doi.org/10.1139/f2011-041>
- Partheniades, E. (2009). *Cohesive sediments in open channels: Properties, transport, and applications*. Burlington, MA, USA: Butterworth-Heinemann.
- Rametter, A. (2007). Multivariate analyses in microbial ecology. *FEMS Microbiology Ecology*, *62*(2), 142–160. <https://doi.org/10.1111/j.1574-6941.2007.00375.x>
- Rautio, M., Mariash, H., & Forsstrom, L. (2011). Seasonal shifts between autochthonous and allochthonous carbon contributions to zooplankton diets in a subarctic lake. *Limnology and Oceanography*, *56*(4), 1513–1524. <https://doi.org/10.4319/lo.2011.56.4.1513>
- Sahoo, G. B., Nover, D., Schladow, S. G., Reuter, J. E., & Jassby, D. (2013). Development of updated algorithms to define particle dynamics in Lake Tahoe (CA-NV) USA for total maximum daily load. *Water Resources Research*, *49*, 7627–7643. <https://doi.org/10.1002/2013WR014140>
- Sillanpaa, M., Neibi, M. C., Matilainen, A., & Vepsalainen, M. (2018). Removal of natural organic matter in drinking water treatment by coagulation: A comprehensive review. *Chemosphere*, *190*, 54–71. <https://doi.org/10.1016/j.chemosphere.2017.09.113>
- Tan, X. L., Zhang, G. P., Yi, H., Reed, A. H., & Furukawa, Y. (2012). Characterization of particle size and settling velocity of cohesive sediments affected by a neutral copolymer. *International Journal of Sediment Research*, *27*(4), 473–485. [https://doi.org/10.1016/S1001-6279\(13\)60006-2](https://doi.org/10.1016/S1001-6279(13)60006-2)
- Tang, F. H. M., & Maggi, F. (2016). A mesocosm experiment of suspended particulate matter dynamics in nutrient- and biomass-affected waters. *Water Research*, *89*, 76–86. <https://doi.org/10.1016/j.watres.2015.11.033>
- ter Braak, C. J. F., & Prentice, I. C. (2004). A theory of gradient analysis. *Advances in Ecological Research*, *34*, 235–282. [https://doi.org/10.1016/S0065-2504\(03\)34003-6](https://doi.org/10.1016/S0065-2504(03)34003-6)
- USEPA. (2002). National water quality inventory: 2000 Report. Washington, DC: EPA-841-R-02-001, Office of Water, U.S. Environmental Protection Agency.
- van der Lee, W. T. B. (2000). Temporal variation of floc size and settling velocity in the Dollard estuary. *Continental Shelf Research*, *20*, 1495–1511.
- van Leussen, W. (1994). Estuarine macroflocs: Their role in fine-grained sediment transport (PhD Dissertation). Utrecht, Netherlands: Utrecht University.
- Weishaar, J., Aiken, G. R., Bergamaschi, B. A., Fram, M. S., Fujii, R., & Mopper, K. (2003). Evaluation of specific ultraviolet absorbance as an indicator of the chemical composition and reactivity of dissolved organic carbon. *Environmental Science & Technology*, *37*(20), 4702–4708. <https://doi.org/10.1021/es030360x>
- Wilkinson, K., Joz-Roland, A., & Buffle, J. (1997). Different roles of pedogenic fulvic acids and aquagenic biopolymers on colloid aggregation and stability in freshwaters. *Limnology and Oceanography*, *42*(8), 1714–1724. <https://doi.org/10.4319/lo.1997.42.8.1714>
- Wisser, D., Frolking, S., Hagen, S., & Bierkens, F. P. (2013). Beyond peak reservoir storage? A global estimate of declining water storage capacity in large reservoir. *Water Resources Research*, *49*, 5732–5739. <https://doi.org/10.1002/wrcr.20452>
- Yang, L., Han, D. H., Lee, B. M., & Hur, J. (2015). Characterizing treated wastewaters of different industries using clustered fluorescence EEM-PARAFAC and FT-IR spectroscopy: Implications for downstream impact and source identification. *Chemosphere*, *127*, 222–228. <https://doi.org/10.1016/j.chemosphere.2015.02.028>

- Yang, L., Hur, J., & Zhuang, W. (2015). Occurrence and behaviors of fluorescence EEM-PARAFAC components in drinking water and wastewater treatment systems and their applications: A review. *Environmental Science and Pollution Research*, *22*(9), 6500–6510. <https://doi.org/10.1007/s11356-015-4214-3>
- Ye, L., Cai, Q., Liu, R., & Cao, M. (2009). The influence of topography and land use on water quality of Xiangxi River in three gorges reservoir region. *Environmental Geology*, *58*(5), 937–942. <https://doi.org/10.1007/s00254-008-1573-9>
- Zhang, G., Yin, H., Lei, Z., Reed, A. H., & Furukawa, Y. (2013). Effects of exopolymers on particle size distributions of suspended cohesive sediments. *Journal of Geophysical Research: Oceans*, *118*, 3473–3489. <https://doi.org/10.1002/jgrc.20263>
- Zhang, Y., Zhang, E., Yin, Y., van Dijk, M. A., Feng, L., Shi, Z., et al. (2010). Characteristics and sources of chromophoric dissolved organic matter in lakes of the Yungui Plateau, China, differing in trophic state and altitude. *Limnology and Oceanography*, *55*(6), 2645–2659. <https://doi.org/10.4319/lo.2010.55.6.2645>
- Zimmermann-Timm, H. (2002). Characteristics, dynamics and importance of aggregates in rivers—An invited review. *International Review of Hydrobiology*, *87*(2–3), 197–240. [https://doi.org/10.1002/1522-2632\(200205\)87:2/3<197::AID-IROH197>3.0.CO;2-7](https://doi.org/10.1002/1522-2632(200205)87:2/3<197::AID-IROH197>3.0.CO;2-7)